Proceedings of ASME Turbo Expo 2011
GT2011
June 6-10, 2011, Vancouver, British Columbia, Canada

GT2011-45113

High Pressure Turbine Low Radius Radial TOBI Discharge Coefficient Validation Process

A.V. MirzaMoghadam, A. Riahi, and M. Morris
Honeywell International
Phoenix, Arizona

ABSTRACT

A TOBI (tangential on board injection) or preswirl system is a critical component of a high pressure turbine cooling delivery system. Its efficient performance and characterization are critical because the blade and disk life depend on the accuracy of delivering the required flow at the correct temperature and pressure. This paper presents a TOBI flow discharge coefficient validation process applied to a low radius radial configuration starting from a 1D network flow analysis to a 3D frozen rotor CFD analysis of the rotor cooling air delivery system. The analysis domain commences in the combustor plenum stationary reference frame, includes the TOBI, transitions to the rotating reference frame as the flow travels through the rotating cover plate orifice, continues up the turbine disk into the slot bottom blade feed cavity, and terminates in the turbine blade. The present effort includes matching a 1D network model with 3D CFD results using simultaneous goal-matching of pressure predictions throughout the circuit, defining test rig pressure measurements at critical "non-disturbing" locations for quanification of pressure ratio across the TOBI, and finally comparing the TOBI flow coefficient resulting from stationary cold flow tests with what was obtained from the 3D CFD results. Analysis of the results indicates that the discharge coefficient varies with pressure ratio and that the traditional method of using a constant discharge coefficient extracted from a cold flow test run under choked conditions leads to over-predicting turbine cooling flows. TOBI flow coefficient prediction for the present study compares well with the stationary data published by author researchers for the configuration under investigation, and the process described in this paper is general for any TOBI configuration.

NOMENCLATURE

A	Correlation multiplier, Fig. 9 and equation 5
A_p	Preswirl geometric flow area, m^2
B	Correlation exponent, Fig. 9 and equation 5
C	Correlation exponent, Fig. 9 and equation 5
C_d	TOBI discharge or flow coefficient
C_p	Specific heat at constant pressure, kJ/kg-K
C_v	Specific heat at constant volume, kJ/kg-K
D	TOBI hole geometric diameter, m
G*	Radial gap ratio between preswirl and receiver surface (s/r_p)
L	Covered length of TOBI orifice, m
$\dot{m}_a$	Actual physical mass flow rate, kg/s
$\dot{m}_i$	Ideal physical mass flow rate, kg/s
P_{ot}	TOBI Inlet total pressure, N/m^2
P_{ref}	Reference test cell pressure, N/m2
P_{1s}	TOBI hole tap pressure (inside orifice), N/m^2
P_{bf}	Blade feed cavity static pressure, N/m^2
$P_{bs,out}$	CFD analysis outlet pressure boundary condition for blade shank cavity, N/m^2
P_{cB}	Cover plate static pressure at bottom of rotating cavity downstream of receiver hole exit, N/m^2
P_{cL}	Cover plate lower cavity static pressure, N/m^2
P_{cM}	Cover plate mid-cavity static pressure, N/m^2
P_{cs}	TOBI exit pressure downstream of orifice, N/m^2
$P_{cs,out}$	CFD analysis outlet pressure boundary condition for compressor flow leakage, N/m^2
P_{cU}	Cover plate upper-cavity static pressure, N/m^2
P_{down}	TOBI downstream pressure, P_{1s} or P_{cs}, N/m^2
$P_{ps,out}$	CFD analysis outlet pressure boundary condition for disk cavity purge flow leakage, N/m^2
P_{ro}	Rotating orifice exit static pressure, N/m^2
P_s	Flow-meter inlet static pressure, N/m^2
P_t	Flow-meter inlet total pressure, N/m^2
r	Radial coordinate
R	Gas constant for a particular gas mixture, J/kg-K
R	Radial coordinate, m
r_p	Centerline radius to TOBI exit, m

S	Distance from TOBI exit to pressure tap P_{1s}, m
s	Radial distance from TOBI exit to rotating surface, m
T_{ot}	TOBI inlet total temperature, K
T_{ref}	Reference test cell absolute temperature, K
T_1	TOBI orifice exit static air temperature, K
T_{1i}	TOBI orifice exit isentropic static air temperature, K
T_t	Flow-meter inlet total temperature, K
V_1	Actual TOBI discharge velocity, m/s
V_{1i}	Isentropic TOBI discharge velocity, m/s
W^*_{corr}	Normalized corrected flow (% maximum corrected flow, $W_c/W_{c,max}$)
W_c	Derived Corrected Flow, $= \dot{m}_a (\sqrt{T/T_{ref}})/(P/P_{ref})$, kg/s
$W_{c,max}$	Derived maximum (i.e. choked) corrected flow, kg/s
X	Axial coordinate

Greek

Δ	Upstream minus downstream
γ	Ratio of specific heats, C_p / C_v
ω	Receiver surface angular speed, rad/s
η_p	Preswirl velocity ratio V_1 / V_{1i}

ABBREVIATIONS

1D	1 dimensional
3D	3 dimensional
CFD	Computational Fluid Dynamics
HPT	High Pressure Turbine
LE	Leading edge of TOBI hole
Poly	Polynomial curve fit
PR	Pressure ratio across TOBI for both sets of flow data, P_{ot}/P_{1s} or P_{ot}/P_{cs} (except where noted)
SR*	Normalized swirl ratio,$[V_1/(r_p\omega)/(\text{design intent})]$
TE	Trailing edge of TOBI hole
TOBI	Tangential On-Board Injection

INTRODUCTION

High pressure turbine cooling delivery systems normally include a mechanism to reduce cooling flow air temperature on board the rotor. One of these mechanisms is the TOBI (tangential onboard injection) system or preswirler which consists of stationary discrete holes or nozzle passage areas angled tangentially in the direction of rotor rotation and oriented parallel (i.e. axial) or normal (i.e. radial) with respect to engine centerline. Aside from shaping the inlet plane to reduce losses, the injection exit plane must meet certain design criteria including optimum distance from the rotating receiving surface, and area ratio between injection flow area and receiver flow area. The performance also depends on the radial position of the TOBI passages with respect to the blade feed holes. The main objective of the TOBI system is to deliver the required cooling flow to the turbine blade and disk cavities in a controlled manner to achieve optimal thermal management satisfying the blade backflow margin (i.e. the ratio of internal cooling passage feed pressure to the external hot flow path pressure). For this critical reason its flow characteristics need to be well understood to ensure successful engine development testing and subsequent operation. Due to a lack of data in low radius radial TOBI systems in the literature as will be shown below, the figure of merit for flow characterization in this study will be the discharge or flow coefficient, defined as the ratio of the actual mass through-flow to the isentropic flow mapped as a function of operating pressure ratio across the TOBI.

TOBI systems work on the basis of accelerating the cooling flow through passages tangentially angled in the direction of rotor rotation. The resulting total temperature in the relative frame of reference as well as the pressure losses encountered entering the receiver/disk hole are reduced due to the achieved high swirl. In 1981, Meierhofer and Franklin [1] were the first to measure the relative cooling air temperature in the rotating blade feed holes of a “direct transfer” system. This configuration lines up the TOBI exit flow with the receiver holes directly feeding the blades in the disk. By its nature, the direct transfer system is an axial TOBI. In 1997, Scricca and Moore [2] additionally reported the “cover-plate” system where the axial TOBI is placed at a lower radius. Upon exiting the preswirl holes, the cooling air flows radially outward between the rotating cover-plate and disk cavity in free vortex manner before entering the blade feed holes in the disk.

In an axial TOBI, there are three main regions/components which influence how efficiently the TOBI delivers the required temperature and pressure to the blades. Referring to Figure 1, these are the TOBI holes (or nozzles), the mixing chamber between stationary and rotating surfaces, and the rotating surface receiver holes. The cover-plate system contributes additional pumping cavity dynamics for the cooling air from where it enters the rotating reference frame at the lower radius receiver holes to where it enters the blade feed holes at the higher radius blade feed slot.

Based on Meierhofer and Franklin [1] work, a linear correlation relating relative temperature drop to preswirler exit-to-receiver hole tangential velocity ratio was obtained. They also defined pre-swirl system performance by the ratio of actual hole/nozzle exit velocity to ideal (or isentropic) velocity. Since it is difficult to measure the “effective” tangential velocity entering the mixing chamber, some researchers such as Dittmann et al. [3] for the TOBI holes, and, Yan et al. [4]

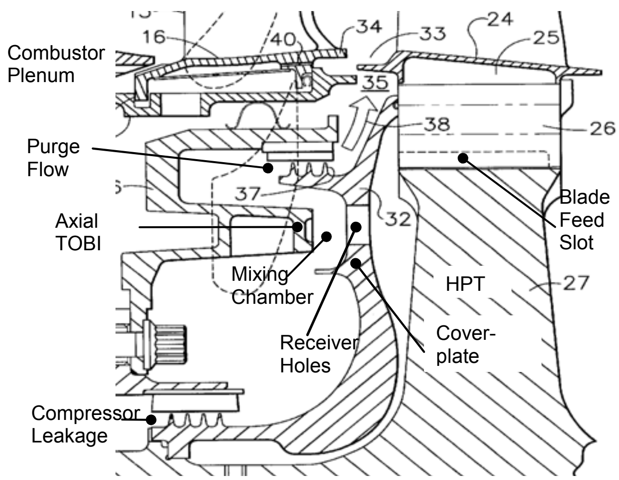

Fig. 1 Axial Preswirl Configuration from Honeywell Patent No. US 6481959B1

and Lewis at al. [5] for the receiver holes, characterized the TOBI system behavior using discharge coefficients. Prior to the work on TOBI system discharge coefficients by these researchers, gas turbine designers were using the discharge coefficients for stationary and rotating holes without pre-swirl application studied by Samoilovich and Morozov [6], Lichtarowitz et al. [7] for incompressible flow, and McGreehan and Schotsch [8]. In addition to the flow characteristics, a recent paper on TOBI system heat transfer behavior by V.U. Kakade et al. [9] reported the effect of radial location of axial pre-swirlers on Nusselt number. In all of the pre-swirl studies cited above, axial TOBI systems were considered. Laurello et al. [10], on the other hand, tested a low radius "radially" oriented pre-swirl system for an industrial gas turbine shown in Figure 2. They demonstrated a reduction in pumping work and an increase in turbine power output by diverting hot compressor leakage flow from passing through the inner nozzle seal and away from the TOBI flow. This eliminated mixing losses and reduced rotor coolant temperature. Since the exit of their radial TOBI was located such that the swirling flow impinged on the receiver surface and then turned axially to flow up the disk surface and into the blade feed holes, pumping power loss was inherently higher due to loss of high pre-swirl in the mixing chamber. They also defined preswirl nozzle losses by the velocity downstream of the exit plane but did not report the actual values.

In assessing the performance of a low radius versus high radius TOBI system, the former can lead to reduced

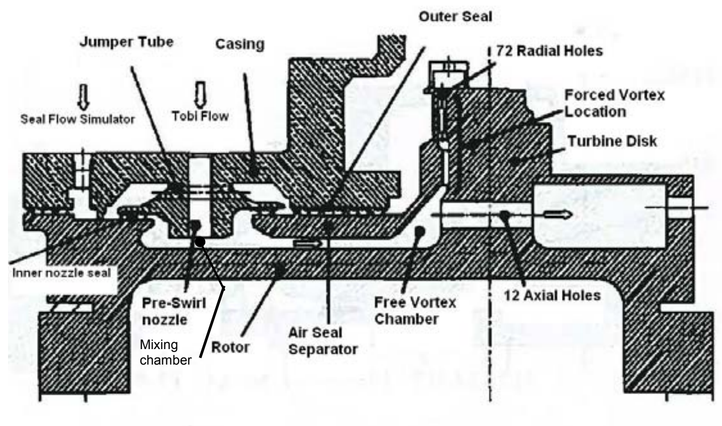

Fig. 2 Radial Preswirl Experimental Rig of Ref. [10]

leakage losses (with additional pumping work) whereas, the latter reduces the cooling air temperature to the blade at the expense of higher leakage. This may also lead to increased aft-directed thrust load. The need for more data and analysis on low radius radial TOBI systems with different designs is evident from the literature search. Beginning with the flow characteristics of the design described in the next section, this paper focuses on the process to validate TOBI discharge coefficients using both computation and cold-flow test rig data.

TOBI DESCRIPTION

The radial TOBI system under consideration in this study is different compared to what has been reported in the literature because it consists of a low radius radial preswirler discharging into a radial receiver hole synchronous with the exit swirl. The configuration is similar to what is shown in Figure 3, and consists of compressor discharge air flowing through the combustor plenum toward the HPT and into discrete radial holes angled tangentially with respect to the direction of disk rotation. The mixing chamber is bounded by leakages flowing forward and aft of the TOBI exit, as well as the radial receiver holes. The aft-directed leakage is the disk cavity purge flow. There are no special chamfering features introduced for the preswirl entrance region. The radial height distance-to-diameter ratio is 1.9 and 0.6 for the TOBI and receiver holes, respectively. The area ratio between receiver and preswirl holes is 3.2. The radial gap ratio G* between preswirl and receiver surface is 0.05. Radial height distance is the radius difference between TOBI exit and receiver hole inlet as seen in a 2D longitudinal view, and diameter refers to the hole. This is in contrast to G* which is the ratio between radial height distance to preswirl exit radius from engine centerline.

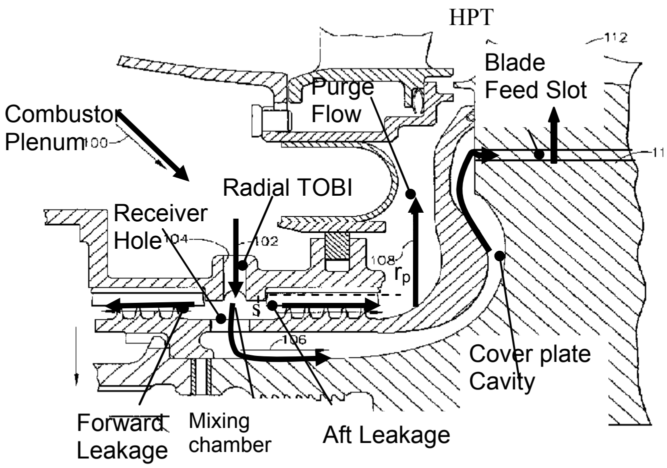

Fig. 3 Radial Preswirl Configuration from Honeywell Patent No. US 6931859B2

The inherent benefit of this TOBI design is the higher than disk speed exit swirl achieved in the mixing chamber such that it remains isolated from any incoming leakage (i.e. from the compressor exit). Moreover, after entering the cover plate cavity, free vortexing to the higher radius decreases the local swirl ratio thereby increasing the relative total temperature; the increase in relative total temperature is reduced by over-swirling the flow at entry to the free vortex cavity. Also, over-swirling helps reduce the pressure drop as the flow enters the blade feed slot.

PROPOSED SCOPE

The accuracy in delivering the required cooling mass flow, relative temperature and pressure to the blade feed slot depends on the following factors defined within the bounds of the TOBI system described in the previous section:

- TOBI inlet pressure, temperature, and swirl velocity (i.e. fluid tangential velocity)
- TOBI inlet-to-exit pressure losses
- Mixing chamber losses
- Forward/Aft labyrinth leakages
- Cover-plate hole losses
- Flow turning losses in the cover-plate cavity
- Cover-plate cavity free vortex effectiveness
- Pressure losses entering the blade feed slot
- Pressure losses entering the blade shank internal cooling channels

The scope of the present work addresses all of the above factors analytically in a deterministic manner. However, the validation of analytical predictions using actual test data is limited to the stationary TOBI discharge coefficient defined by the actual through-flow mass to the ideal (i.e. isentropic) mass flow as defined by equation 1.

$$C_d = \frac{\dot{m}_a}{\dot{m}_i} \qquad (1)$$

The actual mass flow is measured directly in the test, and the ideal mass flow is calculated using the measured pressures. Recently, some researchers such as Bricaud et al. [11] have shown that depending upon where the exit pressure measurements are located, the stationary TOBI discharge behavior may not be influenced by the receiver surface rotational speed. Moreover, they used preswirl velocity ratio to characterize preswirl discharge behavior in lieu of mass flow ratio (i.e. equation 1) as defined by equation 2.

$$\eta_p = \frac{V_1}{V_{1i}} = \sqrt{\frac{T_{ot} - T_1}{T_{ot} - T_{1i}}} \qquad (2)$$

where, V_1 is the discharge velocity, and V_{1i} is the isentropic velocity, where both are determined from the corresponding mass flow assuming negligible density difference between the actual and isentropic states. The corresponding equality with the square root of the temperature difference ratio results from using the energy equation. Although, T_1 and V_1 are related to the mass flow, T_{1i} and V_{1i} are also a function of the pressure ratio across the preswirler. Bricaud et al. indicate that the difference between η_p and Cd is only a few percent according to equation 3.

$$\frac{\eta_p}{C_d} = \frac{T_1}{T_{1i}} \qquad (3)$$

Therefore, in the results section of this paper a comparison is presented between the discharge coefficients obtained for the radial TOBI and η_p corresponding to the axial configuration of Bricaud et al.

VALIDATION PROCESS

The process used to validate the TOBI system consists of two main parts: 1) Perform 3D unsteady/frozen rotor CFD on the geometry configuration of Figure 3, and use area-averaged pressure results at specific locations from TOBI inlet to blade shank feed (see Figure 5) to match the 1-D analytical network tool predictions by adjusting loss/flow coefficients; 2) Conduct cold-flow stationary testing of the preswirler without the rotating receiver holes and compare corrected flow and discharge coefficient with the matched 1-D network model.

1a) The 1-D flow tool used is an in-house computer program called Visual Network, which was described by Ramerth and MirzaMoghadam [12] as also having the capability to perform probabilistic analysis. Step-1 validation process is summarized in Figure 4.

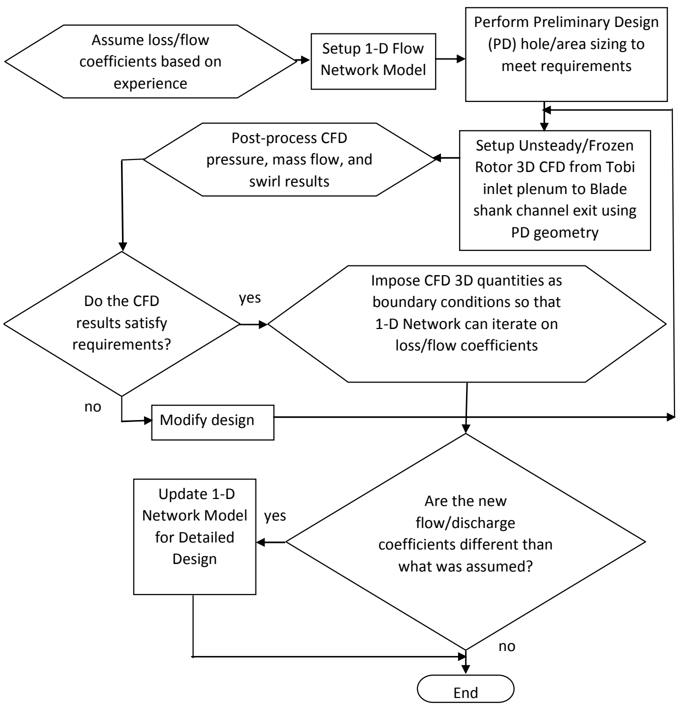

Fig. 4 1-D Network/CFD Validation Process

1b) ANSYS-CFX version 11.0 was used for the TOBI 3D CFD modeling and analysis. Referring to the 2D circumferentially cut view of Figure 5, the analysis domain commenced in the combustor plenum (i.e. inlet cavity) stationary reference frame, includes the TOBI holes, the interface to the rotating reference frame in the mixing chamber, the rotating receiver holes, continues up the turbine disk into the slot bottom blade feed cavity, and terminates in the turbine blade shank feed channels. Boundary conditions included the required TOBI total mass flow into the inlet cavity, and exit static pressures at the forward and aft labyrinth seal locations (see Fig. 3) as well as the blade feed slot, which are shown by arrows in Fig. 5 and labelled "out". The labyrinth seals were simulated with equivalent radial gaps derived from the 1D Network model. The convergence criteria imposed a maximum root mean square value of 1E-04 on the residuals for mass, momentum, and energy. Mesh independent studies (coarse versus fine) were conducted and results compared. The final hexahedra mesh cell count of approximately 2.5 million which evolved from a starting mesh count of 0.25 million, led to less than 0.5% deviation in computed TOBI inlet total pressure with element volume ratio of less than 32 (y plus less than 400). The turbulence model used was the k-epsilon with scalable wall functions. A frozen rotor approach was adopted for the stationary-to-rotating frame change in a 120° periodic sector. Convergence was achieved in approximately 4E+05 computing seconds and 1200 iterations which was equivalent to 1.16 days clock time. The locations (see triangles) where pressure, swirl, and temperature results were extracted from the CFD model to validate the 1-D network model are also shown in Figure 5. A portion of the 120° sector meshed model is illustrated in Fig. 6. This view which represents forward looking aft, includes the TOBI inlet cavity, TOBI holes in the circumferential direction, and the receiver holes.

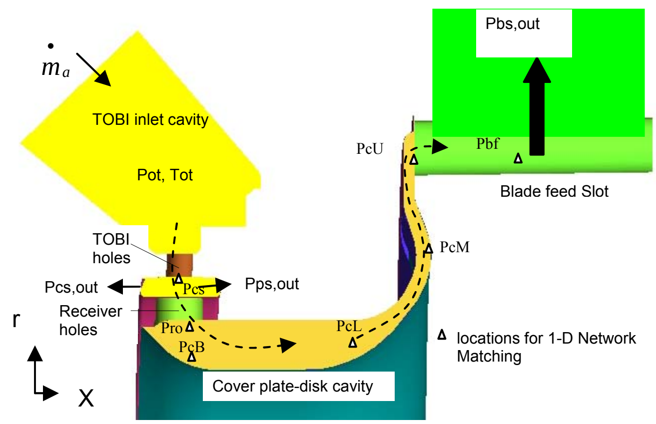

Fig. 5 CFD 2D View Model

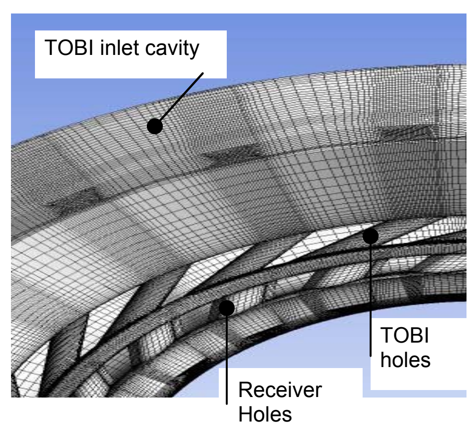

Fig. 6 CFD Sector Meshed Model Looking Aft

2a) <u>Test setup:</u> It is beneficial to validate the through-flow mass of a pre-swirler prior to being installed and tested in the actual engine environment. For this reason, cold-flow testing of the TOBI without the rotating receiver holes is normally performed in a vacuum tank as shown in Figure 7.

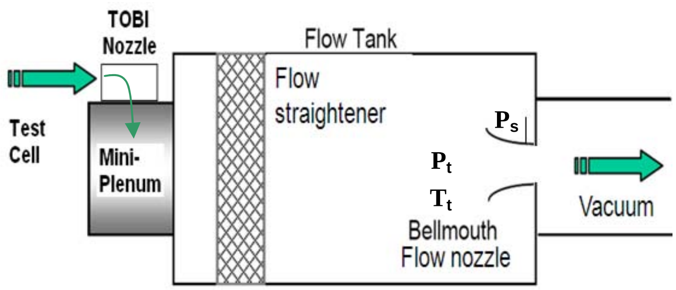

Fig. 7 TOBI Bench Test Apparatus

There are, however, inherent differences between cold flow and engine conditions which need to be considered to correctly characterize the engine TOBI. Most importantly, engine conditions may include time unsteady mass flow behavior not investigated in this paper, whereas the cold flow test is steady. The presence of potential pressure pulsations in the engine condition due to the mismatch in passing frequency between exit flow from the stationary TOBI and receiver hole rotational speed in conjunction with the geometric characteristics may change the flow field in the TOBI holes. This may lead to a change in the TOBI hole vena contracta, which in turn affects the discharge coefficient (and thus the effective area). In order to validate the CFD results, a cold flow test of the actual TOBI part installed on a vacuum tank as shown in Figure 7 was conducted. The direction of the flow from test cell (TOBI inlet) to vacuum pumps has been marked. The vacuum tank is a sealed chamber with an ASME contoured bell-mouth flow nozzle. Prior to test, all pressure transducer modules are calibrated to known reference pressures to ensure data acquisition accuracy.

Figure 8 is the 2D view of Figure 6 at hole centerline axial location. Although, the TOBI was instrumented with two static pressure taps in the inlet plenum located between adjacent TOBI radial inlet holes, the measurement was verified to be the test cell barometric total pressure, and used as P_{ot} in equation 4. Three TOBI holes were instrumented for static pressure measurement (P_{1s}) inside the holes approximately 0.47 diameters (or 25% of the cylindrical length L) upstream of the TOBI hole exit plane. Two static pressure taps (P_{cs}) were placed downstream of the TOBI hole exit plane between adjacent TOBI holes as shown in Figure 8.

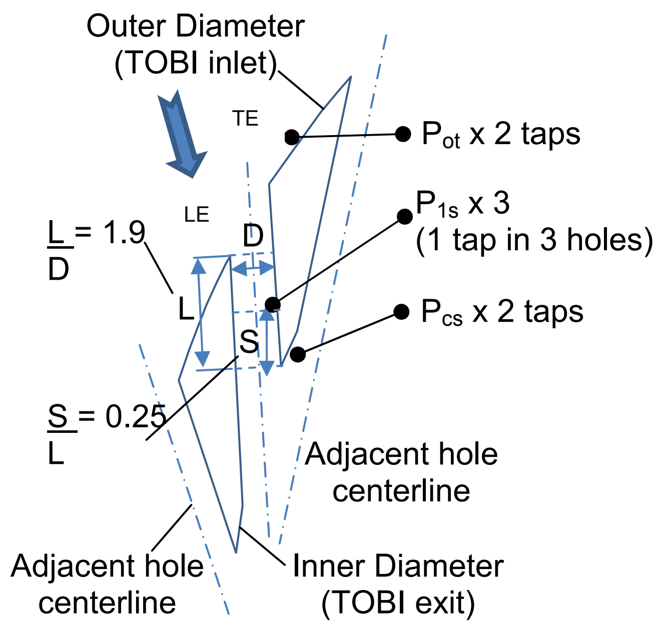

Fig. 8 Location of TOBI Pressure Taps

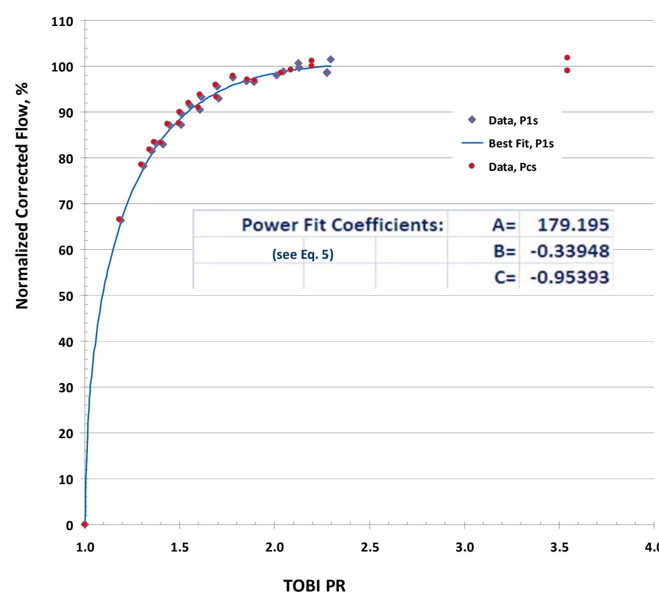

Figure 9 Flow Calibration Curves

2b) <u>Test Conduct:</u>

The through-flow mass as well as total temperature in the inlet plenum was measured against total-to-static pressure ratio across the TOBI holes ranging from 1.0 to 2.3. Prior to testing, a leak check was performed and no leaks were detected. The test was conducted by continuously pulling vacuum in the tank and recording mass flow through the system until no additional flow increase occurred in the TOBI (choked flow). The instrumentation enabled the generation of a flow calibration curve, shown in Figure 9, which relates the normalized measured corrected flow ($W_c/W_{c,max}$) to the measured pressure ratio based on the TOBI inlet pressure P_{ot} to the two pressure tap locations P_{1s} (in the TOBI hole) and P_{cs} (downstream of the TOBI hole exit). After reaching a pressure ratio of 2.3, the measured flow remained constant to within ±1%. At low pressure ratios, the TOBI orifice pressure P_{1s} tracks well with the downstream exit pressure P_{cs}. At large pressure ratios, however, the pressure inside the TOBI holes P_{1s} asymptotically approaches a constant value (within the experimental uncertainty) as is also shown by the blue curve in Fig. 10. Thus, at larger pressure ratios, the TOBI orifice pressure P_{1s} diverges from the TOBI exit pressure P_{cs}. The pressure difference plot of Figure 9 (red curve) illustrates this observation. As expected, the pressure P_{cs} downstream of the TOBI exit continues to fall as it tracks the downstream vacuum tank pressure. Data acquisition stopped at a value corresponding to a pressure ratio of 3.55 as shown in Figures 9 and 10. Note that the TOBI orifice pressure location P_{1s} was instrumented with three pressure taps (one tap in three individual TOBI holes) as shown in Figure 8, due to its strategic location. This enabled a more robust flow calibration characterization of the TOBI by allowing uncertainty in measurements to be captured by redundancy. Data acquisition was conducted at room temperature and at stationary, steady state conditions. Data reduction included using equation 4 (from reference [3] for stationary nozzles) with the measured actual mass flow, pressure ratio (per the measured locations shown in Fig. 8), and total temperature to derive TOBI discharge coefficient.

$$C_d = \frac{\dot{m}_a}{\dot{m}_i} = \frac{\dot{m}_a}{\dfrac{A_P P_{ot} \sqrt{\dfrac{2\gamma\left(\left(\dfrac{P_{1s}}{P_{ot}}\right)^{\frac{2}{\gamma}} - \left(\dfrac{P_{1s}}{P_{ot}}\right)^{\frac{\gamma+1}{\gamma}}\right)}{\gamma - 1}}}{\sqrt{RT_{ot}}}} \qquad (4)$$

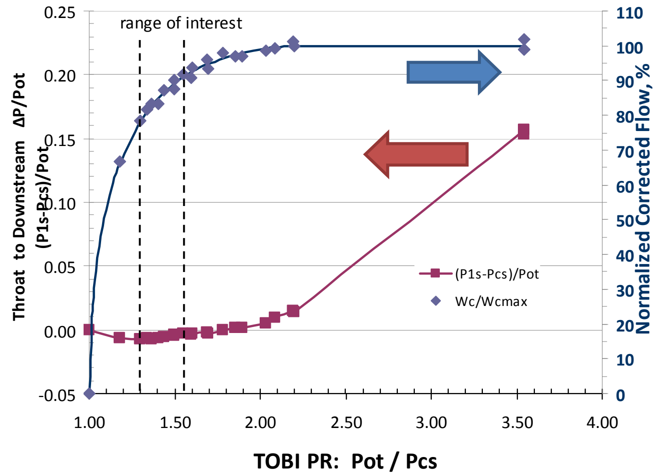

Fig. 10 Flow Calibration Curves

2c) <u>Error Analysis</u>

The bell-mouth nozzle flow accuracy is between ±0.5% to ±1.0%. All pressure readings are accurate to ±0.25% full scale. The errors for the corrected flow (W_c), pressure ratio (PR), and discharge coefficient (C_d) were calculated using the method of Kline and McClintock [13]. These turned out to be +/-0.74% for W_c, +/-0.30% for PR, and +/-0.79% for C_d.

VALIDATION RESULTS AND DISCUSSION

Detailed study of the CFD flow field through the TOBI holes was conducted. This allowed a better understanding of what to expect from the test data at subsonic pressure ratios. Firstly, the shape and profile of the vena contracta area upon entering the preswirler was determined using vector plots colored by pressure. Referring to Figure 11, the radial-tangential view through the hole illustrates the skewed entrance characteristic of the flow biased toward the trailing edge (TE) where pressure losses are lower than along the leading edge surface. The vena contracta area appears to reach its minimum toward the exit. Secondly, the location of P_{1s} pressure tap downstream of the hole inlet for the test which was shown in Fig. 8, is represented by the circular plane of the hole cross-section in the CFD pressure contour plot of Figure 11.

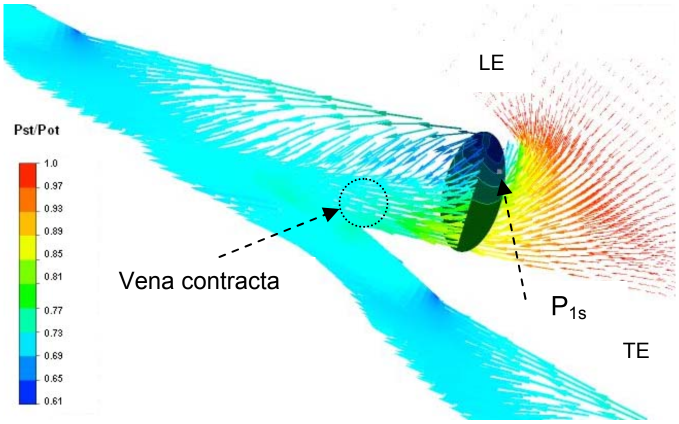

Fig. 11 TOBI hole flow field and location of P_{1s}

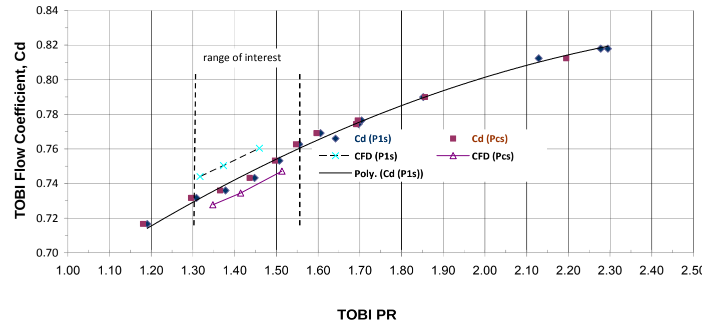

Fig. 12 Test Data versus CFD TOBI Discharge Coefficients

The contours on the illustrated P_{1s} plane located at an S/D ratio of 1.4 (rather than the tested 0.47 herein) show that if the tap had not been located further downstream inside the hole, it would be more susceptible to disturbances caused by a high gradient area (refer to Fig. 6 for hole orientation).

Referring to Figure 9, the corrected flow versus pressure ratio based on the two TOBI pressure measurements P_{1s} and P_{cs} illustrate rig sensitivity to flow characterization. For the pressure ratio range of interest, the two pressure measurement locations do not show an appreciable deviation, but at higher pressure ratios, there is a deviation of about 2%. The location P_{1s} inside the TOBI hole, therefore, shows more stability from downstream pressure changes as noted earlier, see Figure 10. All data correlate well with a power law expression on normalized corrected flow defined by equation 5 valid for subsonic pressure ratios.

$$\overset{*}{W}_{corr} = 179.2PR^{-0.34}\sqrt{1-(PR)^{-0.954}} \qquad (5)$$

Nevertheless, the difference in TOBI discharge coefficient versus pressure ratio is minimal for the two locations across the tested pressure ratio range as presented in Figure 12. Another interesting result is that the discharge coefficient continuously varies with pressure ratio even at the high values. This implies the over-estimation of TOBI discharge coefficient when it is derived based on sonic conditions.

In order to validate the slope of the discharge coefficient curve shown in Figure 12 in the vicinity of the pressure ratios of interest (e.g. 1.3-to-1.55), the CFD model was rerun at two additional points (higher and lower pressure ratios). Those points are also shown in Figure 12, and magnified in Figure 13 representing the two pressure measurement locations P_{1s} and P_{cs}. Although the CFD predictions exhibit a slope similar to the test data, the deviation of the inside P_{1s} and outside P_{cs} hole pressure measurement locations is larger than what the test data revealed. In this case, it is respectively within ±1.35% of the curve fitted data in Figure 12. The CFD results also show that the exit location P_{cs} has a lower pressure compared to that inside the hole at location P_{1s}, which is contrary to what was measured in test at this range of pressure ratios. Although, these differences could be attributed to the effects of a rotating surface which is absent in the cold flow test data, after reaching a pressure ratio of 1.9, however, the test data confirm that the outside pressure P_{cs} begins to drop more than the TOBI inside location P_{1s}.

The increasing trend in TOBI discharge coefficient with pressure ratio (albeit, the slope is decreasing at the higher pressure ratios) was also observed by Dittmann et al. [3] and more recently, by Bricaud et al. [11] for axial TOBI configurations. The former compared their stationary inlet-chamfered hole test-rig to the CFD rig-model across a range of pressure ratios and obtained discharge coefficients using equation 4. The latter obtained test data and TOBI flow discharge coefficients by varying hole radius as well as mixing chamber size/geometry for both straight and chamfered inlet holes using equation 2. Figure 14 shows the comparison between the present study and the work of these researchers including a comparison of the two sources on a chamfered inlet hole configuration. The measurement error reported by these researchers for the discharge coefficient is in the order of +/-0.7% which is in the same order as this study (i.e. 0.79%). Firstly, the data shows reasonable agreement between the straight hole results of this study and that by Bricaud et al. which improves as the pressure ratio increases (deviation is 4% at PR of 1.2, 0.7% at PR of 1.6, average deviation is about 2% across the commonly tested PR). In addition, raising the preswirler discharge coefficient (in the order of 20%) can be achieved by chamfering the inlet as demonstrated by other researchers. Secondly, this study has investigated a radial preswirler, whereas, the literature tested a high radius axial preswirler. Considering an averaged deviation of 2% for a straight hole at low pressure ratio between this study and that of Bricaud et al. along with a representative experimental error of +/-0.75% between the two studies, one may conclude that the TOBI configuration (i.e. axial versus radial) and methodology (i.e. velocity ratio versus mass flow ratio) accounts for a total of about 0.5% error on average and 2.5% at maximum. Therefore, to arrive at a reasonably accurate discharge coefficient irrespective of TOBI configuration and methodology described herein, it is necessary that the pressure measurements be taken inside or near the exit plane. This is an important contribution from this study.

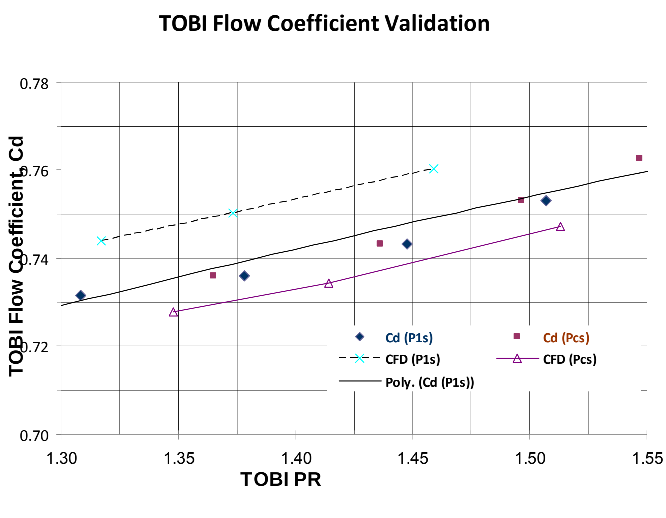

Fig. 13 Test Data versus CFD TOBI Discharge Coefficient in the Vicinity of the Pressure Ratio of Interest

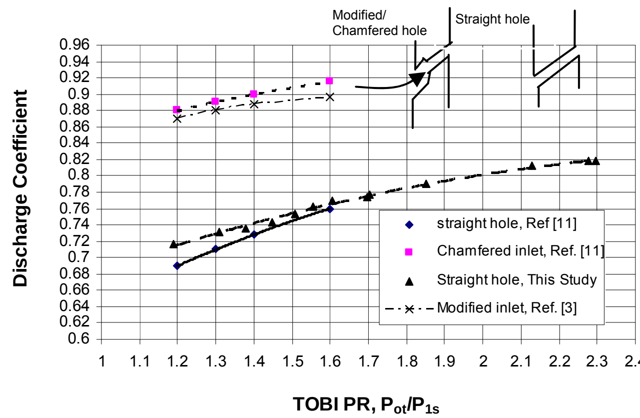

Fig. 14 Test Data versus Literature

The lower discharge coefficient resulting from a straight machined preswirl hole has an adverse effect on maximum achievable swirl ratio because the required blade flow for thermal management will necessitate increasing hole size. This in turn, will increase the air relative temperature feeding the blade. On the other hand, reducing the inlet turning losses to the preswirl hole by machining a larger entrance coincident with the flow turning angle will substantially improve discharge coefficient leading to a reduction in geometric area and improving exit swirl. Figure 15 presents the variation in swirl ratio along the straight preswirl hole (refer to Fig. 6 for hole geometry/orientation). It is clear that the low discharge coefficient has also limited the maximum achievable swirl ratio even without resizing.

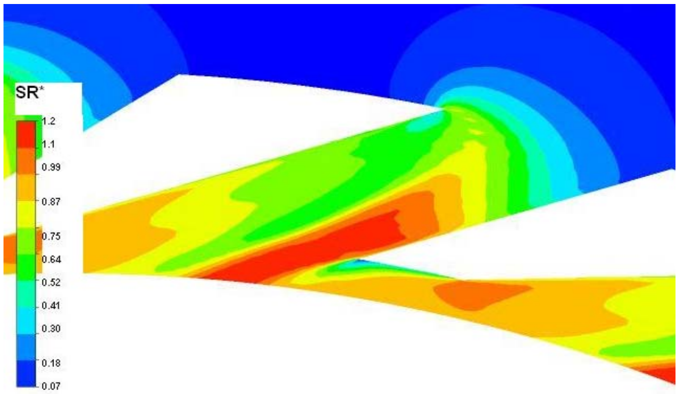

Fig. 15 Contours of TOBI Swirl Ratio

CONCLUSIONS

There is a performance parameter which is associated with the pressure-to-kinetic energy conversion efficiency across the TOBI stationary hole. This is the discharge coefficient (or flow coefficient) defined by either the ratio of the actual-to-ideal through-flow mass or the ratio of the actual-to-ideal exit velocity.

This study has shown that the difference in discharge coefficient using the radial configuration with mass flow versus the axial configuration with velocity is within 2%. It has also contributed by expanding the database on straight hole TOBI discharge coefficient up to a pressure ratio of 2.3. The increasing trend with pressure ratio continues beyond the theoretical sonic pressure ratio of 1.89. The increase in discharge coefficient in the subsonic regime may occur because of the reduction in the inlet vena contracta area due to compressibility effects. Beyond the theoretical sonic pressure ratio, however, flow has not yet reached its maximum value until a pressure ratio of 2.3. This was attributed to the non-ideal shape of the TOBI hole due to its tangential angle. Beyond this ratio, the mass flow remains constant as does the TOBI hole pressure ratio based on P_{1s}; whereas, the TOBI exit pressure P_{cs}, which is decoupled from the TOBI hole fluid dynamics, continues to drop. Based on this observation, the optimum pressure measurement location is recommended to be inside the hole but sufficiently downstream of the inlet to be clear from inlet losses/disturbances which for this study is at S/D=0.47 or 75% downstream of the LE inlet.

REFERENCES

[1] Meierhofer B., and Franklin C.J., 1981, "An Investigation of Preswirled Cooling Airflow to a Turbine Disk by Measuring the Air Temperature in the Rotating Channels", ASME Paper # 81-GT-132

[2] Scricca J.A., and Moore K.D., 1997, "Effects of "Cooled" Cooling Air on Pre-Swirl Nozzle Design", Tech. Report NASA/CP-98-208527, Pratt & Whitney.

[3] Dittmann M, Geis T., Schramm V., Kim S., and Wittig S., 2001, "Discharge Coefficients of a Pre-Swirl System in Secondary Air Systems", ASME Paper # 2001-GT-0122.

[4] Yan Y., Farzaneh-Gord M., Lock G.D., Wilson M., and Owen J.M., 2003, "Fluid Dynamics of a Pre-Swirl Rotor-Stator System", ASME J. of Turbomachinery, 125, pp. 641-647.

[5] Lewis P., Wilson M., Lock G.D., and Owen J.M., 2007, "Physical Interpretation of Flow and Heat Transfer in Pre-Swirl Systems", ASME J. of Engineering for Gas Turbines and Power, 129, pp. 769-777.

[6] Samoilovich G.S., and Morozov B.I., 1957, "Coefficients of Flow Through Pressure Equalizing Holes in Turbine Disks", Teploenergetica, 8, pp.16-23.

[7] Lichtarowicz A., Duggins R., and Markland E., 1965, "Discharge Coefficients for Incompressible Non-Cavitating Flow Through Long Orifices", Journal of Mechanical Engineering Science, 7(2), pp. 210-219.

[8] McGreehan W.F., and Schotsch M.J., 1987, "Flow Characteristics of Long Orifices With Rotation and Corner Radiusing", ASME Paper # 87-GT-162.

[9] Kakade V.U., Lock G.D., Wilson M., Owen J.M., and Mayhew J.E., 2009, "Effect of Radial Location of Nozzles on Heat Transfer in Pre-Swirl Cooling Systems", ASME Paper # GT2009-59090.

[10] Laurello V., Yuri M., Fujii K., Ishizaka K., Nakamura T., and Nishimura H., 2004, "Merasurement and Analysis of an Efficient Turbine Rotor Pump Work Reduction System Incorporating Pre-Swirl Nozzles and a Free Vortex Pressure Augmentation Chamber", ASME Paper # GT2004-53090.

[11] Bricaud C., Geis T., Dullenkopf K., and Bauer H.-J., 2007, "Measurement and Analysis of Aerodynamic and Thermodynamic Losses in Pre-Swirl System Arrangements", ASME Paper # GT2007-27191.

[12] Mirzamoghadam A.V., Ramerth D.L., Kiratsingh A., and Banda G., 2010, "A Probabilistic Secondary Flow System Design Process for Gas Turbine Engines", ASME Paper # GT2010-22071, Accepted for Publication in Journal of Engineering for Gas Turbine and Power.

[13] Kline, S.J., and McClintock, F.A., "Describing Uncertainties in Single-Sample Experiments", Mech. Eng., vol.75, January 1953.